A. Rizzi, M. Tomac, A. Jira¡sek, L. Cavagna, L. Riccobene, S. Ricci
Computation of Aeroelastic Effects on F-16XL at flight conditions FC70 and FC25
Journal of Aircraft, Vol. 54, N. 2, 2017, p. 409-416
doi:10.2514/1.C033227

Computation of Aeroelastic Effects on F-16XL at Flight Conditions FC70 and FC25

Arthur Rizzi* and Maxmilian Tomac†
Royal Institute of Technology, 100 44 Stockholm, Sweden
Adam Jirásek‡
The Swedish Defence Research Agency, 164 90 Stockholm, Sweden
and
Luca Cavagna,§ Luca Riccobene,§ and Sergio Ricci¶
Politecnico di Milano, 20156 Milano, Italy

DOI: 10.2514/1.C033227

This article presents an aeroelastic study of CAWAPI F-16XL aircraft. The structural model of this aircraft is not publicly available and is therefore replaced by a structural model estimate that is constructed based on data available in public literature. The aeroelastic solution is done using solution for two flight conditions — FC70 and FC25. The primary task is to assess the importance of the aeroelastic effects on the FC70 solution and to assess whether large discrepancies are observed at flight condition FC70 between the computational and experimental data.

I. Introduction

THE CAWAPI F-16XL has been extensively studied in the past [1–7]. The primary focus of the previous studies was the vortical flows around the delta wing of this aircraft at lower Mach numbers using different turbulence models and steady and unsteady modeling. One of the selected conditions was, however, a flight at high Mach number and low angle of attack. This condition was considered a simpler one because low angle of attack proved to be the most troubling with large discrepancies between the numerical modeling and flight data. Although the differences between computational fluid dynamics (CFD) codes were smaller than those for all other conditions, the comparison to the flight data was the worst. A number of studies were carried out in order to track the origin of the differences for the flight conditions as reported in [3], mainly the study of different turbulence models, study of computational mesh effect, and modeling of deflected controls, but none of these was able to definitely determine the cause.

In their introductory paper to CAWAPI-2, Luckring et al. [8] reiterate that possible aeroelastic deflections of the airframe (outer wing panel) due to the high dynamic pressure could be the cause of the discrepancy. And they call for strategies to put in place approaches that will take aeroelastic deflections into account. One strategy could be just a rough first-order estimate of the aeroelastic effects associated with the high dynamic pressures of the transonic flight conditions. It can only be a tough estimate because only limited knowledge about the structural model of the aircraft is available, but this approach can give a sense of whether elastic effects move the rigid CFD in the direction of the flight measurements that could still be useful. That is exactly the approach taken in this paper and its overall objective.

All previous studies of F-16XL were carried out assuming that the aircraft is rigid. This was done partly to avoid the additional complexity due to modeling of aeroelastic effects but mainly because the necessary details about the aircraft structure are missing (e.g., its modal characteristics). Moreover, the possible aeroelastic effects were deemed to have small effect. But when all other attempts failed to identify a possible cause for the discrepancy between computed results and flight data, attention turned to evaluating the previously omitted aeroelastic effects. The structural model of the aircraft, however, is not publicly available; thus, the team needed to devise a means to "bootstrap" an approximate model that was carried out in the following way. Next-generation Conceptual Aero Structural Sizing (NeoCASS) [9] is a free suite of Matlab modules that combines state-of-the-art computational, analytical, and semiempirical methods to tackle all the aspects of the aerostructural analysis of a design layout at the conceptual design stage (www.neocass.org). There is sufficient information about the F-16XL available in the public literature to initiate a conceptual design layout of the aircraft with NeoCASS, which will result in, for example, a stick-beam model of the structure that is sized for the expected aerodynamic loading. Moreover, results of the ground vibration tests of the F-16XL have been published against which the NeoCASS model can be "tuned" to improve its accuracy. And from this tuned NeoCASS model, a reasonably accurate modal representation of actual structural model of the full aircraft can be obtained. Then this modal representation is used in the CFD solver Edge to carry out the aeroelastic analysis at transonic speed. That is the strategy followed in this paper.

The results of the Edge aeroelastic analysis of the F-16XL aircraft with the designed approximation of the structural model indicate that the aeroelastic effect at this flight condition has a moderate effect on solution. Despite some visible changes in pressure distribution on the wing, the overall character of the flowfield remains unaffected, and it was therefore concluded that omission of the aeroelastic effect of the aircraft is not a cause to limited accuracy of the numerical analysis of this aircraft.

The paper is structured in the following way. Section II presents the publicly available data that are used in NeoCASS to carry out the structural sizing and modal structure. Section III develops the modal estimate and tunes it with the ground vibration test data. Section IV describes the Edge code and compares surface c_p values computed for FC70 and FC25 with the flight test measurements. Finally, Sec. V draws some conclusions from the comparisons.

Presented as Paper 2014-0421 at the 52nd Aerospace Sciences Meeting, National Harbour, MD, 13–17 January 2014; received 11 October 2014; revision received 26 March 2015; accepted for publication 10 June 2015; published online 21 July 2015.

*Professor, Department of Aeronautical and Vehicle Engineering. Associate Fellow AIAA.

†Ph.D. Student, Department of Aeronautical and Vehicle Engineering. Associate Fellow AIAA.

‡Senior Research Scientist, Department of Systems Technology. Senior Member AIAA.

§Researcher, Dipartimento di Scienze e Tecnologie Aerospaziali, Politecnico di Milano.

¶Associate Professor, Dipartimento Scienze e Tecnologie Aerospaziali, Politecnico di Milano. Member AIAA.

Table 1 F-16XL-1 airplane specifications [1]

Feature	Value
Wing span	32.4 ft
Height	17.606 ft
Length	54.155 ft
Reference chord	24.7 ft
Theoretical root chord	41.75 ft
Wing area	646.37 ft^2
Reference wing area	600 ft^2
Reference aspect ratio	1.75
Typical takeoff weight	35,000 lb
Engine max thrust Pratt & Whitney F100-PW-200	23,830 lb

II. F-16XL CAWAPI Aircraft Description

The F-16XL-1 airplane is an aircraft developed by the General Dynamics Corporation — by stretching the fuselage of a full-scale F-16A and adding a cranked-arrow wing. There were two F-16XL aircraft built: F-16XL-1 was used in the CAWAPI, and F-16XL-2 was a two-place version. Both aircraft have leading-edge flaps, elevons, and ailerons on the wing. The technical specifications of the airplane are given in Table 1 of [1]. The design of the cranked-arrow wing was a cooperative effort of the NASA Langley Research Center and the General Dynamics Corporation. The new wing was designed to provide the F-16 aircraft with improved supersonic performance while maintaining comparable transonic performance to that provided by the current F-16 design. As shown in Fig. 1, the final design had a leading-edge sweep angle of 70 deg inboard and 50 deg outboard of the crank with S-blend curve at the wing leading-edge fuselage junction, which was designed to alleviate a pitch instability at high angles of attack [1]. The wing is equipped with the air-dam fence and wing-tip missiles.

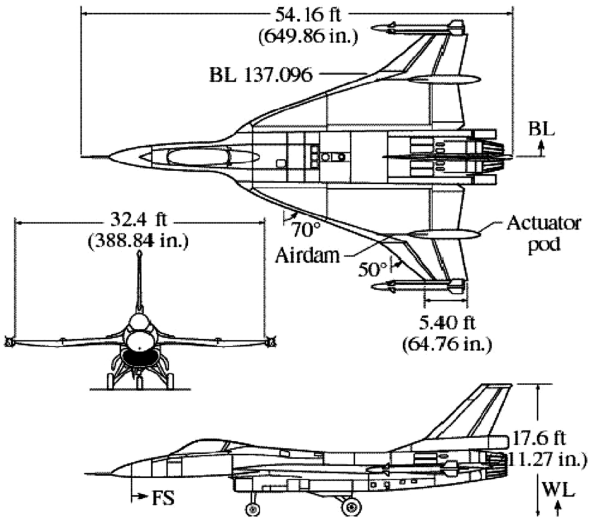

Fig. 1 F-16XL-1 airplane [1].

III. Aeroelastic Model Estimate

The aeroelastic model of F-16XL has been designed using the typical approach that is used during the aircraft conceptual design. For this purpose, dedicated software called NeoCASS was used.

NeoCASS [9] was originally developed during the FP6-SimSAC project, and since 2011 it has been an open source project (www.neocass.org). It is a suite of modules that combine state-of-the-art computational, analytical, and semiempirical methods to address all aspects of the aerostructural analysis of the design at a conceptual design stage. It gives quick understanding of the problem without neglecting any aspect of it: the weight estimate, initial structural sizing, aerodynamic performances, structural and aeroelastic analysis from low to high flight speeds, divergence, flutter analysis, and determination of trimmed condition and aerodynamic derivatives both for the rigid and elastic aircraft. The NeoCASS includes three main modules: the Generic Unknowns Estimator in Structural Sizing (GUESS), the Simplified Models for Aeroelasticity in Conceptual Aircraft Design (SMARTCAD), and the Weight and Balance (W&B).

The W&B module is a lookup table module and is used by GUESS to produce the first estimate of the nonstructural masses and their location for the estimate of inertial loads. This guess is based on data sheets. The semianalytical module GUESS then estimates the stiffness distribution for entire airframe based on user-defined sizing maneuvers. The structural sizing of GUESS model produces a reasonable stiffness distribution and improved estimate of the primary structural masses from W&B module results. The module automatically generates the structural and aerodynamic computational meshes for subsequent numeric aeroelastic assessment and optimization done in SMARTCAD.

The SMARTCAD module is a numerical module dedicated to the aerostructural static and dynamic analysis. In NeoCASS, two reduced-order models are available: a linear/nonlinear finite-volume beam and a linear equivalent plate model, which will be briefly presented in the following sections. The two structural models have been used to produce a realistic aeroelastic model of F-16XL aircraft by running a two-step procedure. As an input, the module uses publicly available F-16XL data given in Table 1.

A. Initial Structural Model

The initial structural model has been generated using the standard procedure implemented in NeoCASS and a stick-beam model. The user then selects a set of sizing maneuvers and the module computes the aerodynamic loads using low-fidelity aeromodeling such as the vortex lattice method or the double-lattice method. The aerodynamic loads are then transferred from the aerodynamic surface to the stick model. Finally, the structural properties of each section of the beam model are determined using an optimization procedure with struc-

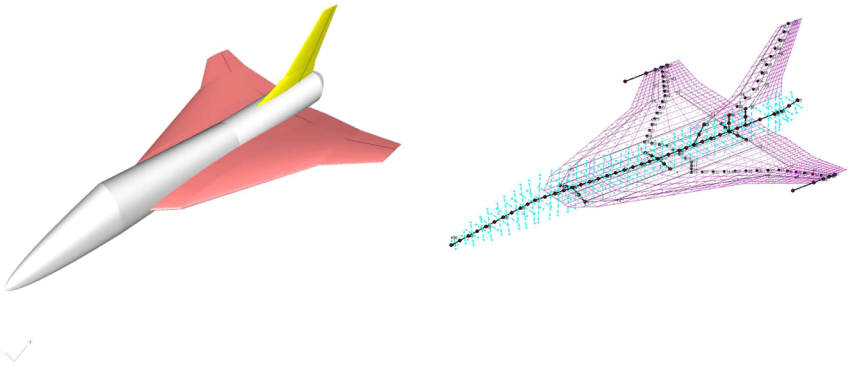

a) Aircraft geometry **b) Aircraft aeroelastic model**

Fig. 2 F-16XL geometry (left) and aeroelastic model (right).

Table 2 Estimated modes from NeoCASS

Mode	Measured, Hz	Hybrid, Hz, GUESS sizing	Hybrid, Hz, after updating
1st bending (symmetric)	7.98	17.48	7.98
1st bending (antisymmetric)	10.79	18.73	8.13[a]
1st bending fin	12.48	26.39	12.4
1st torsion (symmetric)	13.70	54.77	13.70

[a]Mode not included in the updating process.

tural constraints such as maximum stresses and instability constraints.

With a minimal intervention by the user, the NeoCASS software is able to generate a realistic stick model of a complete aircraft, including all data necessary for definition of the fluid–structure interface. The stick model is based on a finite-volume nonlinear beam model that is very efficient and especially suitable for medium- to high-aspect-ratio aircraft. For an aircraft with low-aspect-ratio wing, such as F-16XL, a more suitable structural model based on the linear equivalent plate model is available. Figure 2 shows the geometrical model of F-16XL created inside AcBuilder, the standard preprocessor of NeoCASS together with the stick model created during the first sizing loop. The initial stick model was constructed using elevons surfaces to control trim in pitch; the aerodynamic model of the fuselage is not considered. The maximum take off weight mass without weapons and under-wing stores was set to 12,196 kg, along with three sizing maneuvers at a fixed altitude of 1524 m and at flight Mach number $M = 0.304$ corresponding to flight condition FC7, which should generate large values of the dynamic pressure [2,10,11]. The three sizing maneuvers are a pull-up with positive normal load factor of $9g$, a pull-up with negative load factor of $-3g$, and an abrupt rudder deflection of 25 deg; the first two symmetric maneuvers are used for sizing the airframe, and the last one is needed to design a sufficiently stiff fin.

B. Final Structural Model

As mentioned above, NeoCASS offers a second structural model based on the equivalent plate concept. The equivalent plate is a reduced-order structural model that can represent a simple plate or a wing box, including spars, stringers, and ribs. Wing planform and structural layout depend analytically on a small set of shape and sizing design variables. The model generation is fast compared with the detailed finite-element model, and the aeroelastic optimization problem is formulated using a small number of variables that improve the speed of the optimization. Using the Ritz approximation, the displacements are given by a series of functions defined over large portions of the wing. Stress recovering, concentrated force/moment application, and structural and aerodynamic grid interpolation are straightforward. However, the Ritz coordinates do not have the same physical meaning of the finite-element nodal degrees of freedom, which represent three displacements and three rotations, and a space coordinate transformation is therefore needed, especially when coupling the Ritz model with FEM codes.

Despite some known drawbacks, the equivalent plate method is suitable for the conceptual design phase, in which many different aircraft layouts have to be examined and the primary concern is a reasonable structural weight estimate. Besides for flying wings, in which it can be used directly, the implementation of a hybrid model, which combines beams and plates, allows treating the general aircraft configurations [12]. The strategy adopted in this work for the definition of the aeroelastic model of F-16XL is based on the above-mentioned hybrid model, in which the wing and vertical tail are treated as equivalent plates, while the fuselage and the launching rails are modeled as beams. Using the preliminary structural stick model as a starting point, the final structural properties were computed by means of a modal tuning process that tries to match the first frequencies and mode shapes with the data measured during a modal testing flutter campaign [13].

The tracking process is driven by a gradient-based optimization coupled with a modal assurance criterion (MAC) to prevent mode switching. Thirteen plates are used to model the lifting surfaces — 10 for the wing and 3 for the fin — and the corresponding equivalent thicknesses are the design variables, updated during the optimization problem. Because the aircraft is symmetric, the number of variables is reduced to 8 (5 for the wing and 3 for the fin); upper and lower bounds are applied to avoid unfeasible solutions. The objective function is the sum of the differences between the target frequencies and the actual frequencies, weighted on the maximum difference (thus, the higher the computed frequency, the higher the weight). Because the target is given in terms of frequency, during the updating process mode switching is likely to occur; this is a common issue in structural optimization problems [14,15] and different methods are available to correlate target shapes with actual shapes.

In the present work, a MAC-based mode tracking (similar to cross-orthogonality check) is used: when tracking a single mode, the highest MAC index, that is, the index closer to unity, between the actual shapes and target shape identifies mode position within the modal base, and thus the frequency vector is rearranged to correctly compute weights and differences. As can be seen in Table 2, by starting from a very stiff airframe coming from GUESS initial sizing, the method devised provides a very good agreement with target modes, except for the first antisymmetric bending mode that shows a 25% error. The similarity of shapes for the antisymmetric bending mode and the fin-bending mode slowed the convergence, and the first bending (antisymmetric) mode has therefore been excluded from the tracking process, favoring the correct mode sequence over global accuracy. Because FC70 and F25 are symmetric flight conditions, this seems to be a reasonable action. Figures 3 and 4 show measured [13] and NeoCASS-predicted symmetric and asymmetric bending and torsion modes that were used in the tracking process described above.

IV. High-Fidelity Coupled Aeroelastic Simulations

The NeoCASS modeling is for linear aerodynamics and structures, that is, midfidelity, and so, to analyze transonic aeroelastics, the NeoCASS modal structure must be input to the high-fidelity CFD code Edge to model the static aeroelastic deformation of the CAWAPI

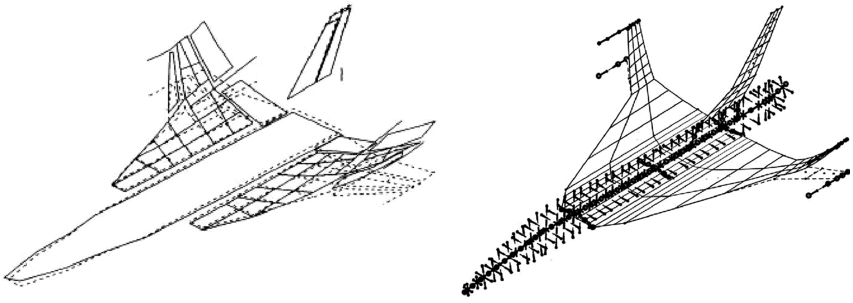

Measured Predicted

Fig. 3 Symmetric bending mode 7.98 Hz: dashed line, rigid shape; solid line, mode shape.

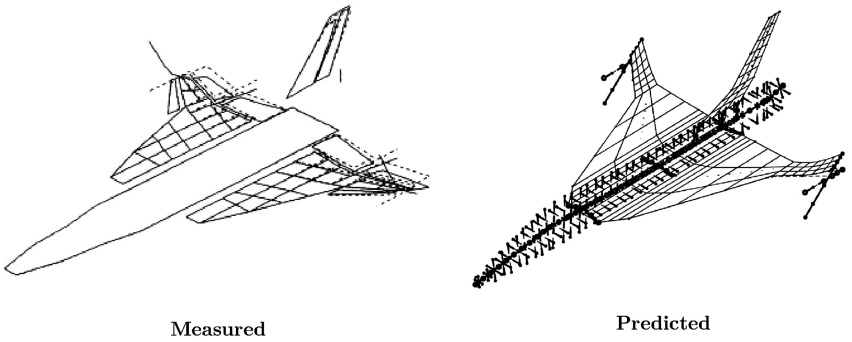

Measured Predicted

a) Symmetric torsion mode 13.69 Hz

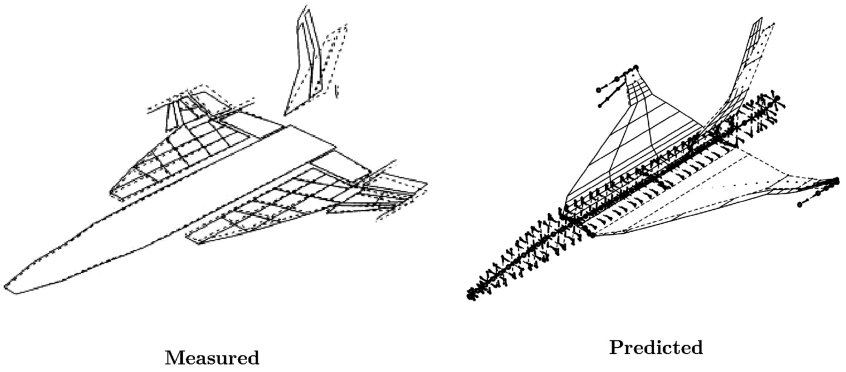

Measured Predicted

b) Asymmetric torsion mode 12.48 Hz

Fig. 4 First torsion mode shapes: dashed line, rigid shape; solid line, mode shape.

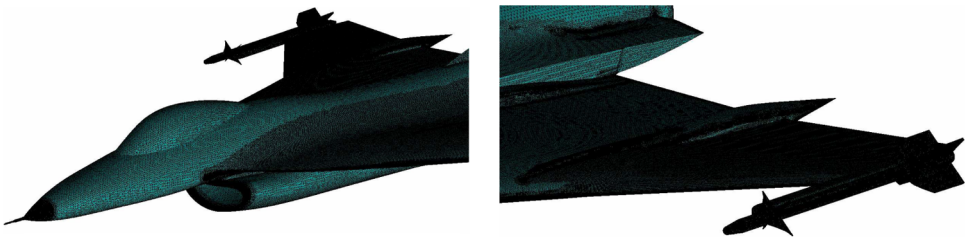

a) Detail of the viscous mesh **b) Detail of the viscous mesh**

Fig. 5 Viscous computational mesh on the surface of the aircraft.

F-16XL configuration at the transonic flight condition FC70, namely, Mach number $M = 0.97$, angle of attack $\alpha = 4.37$ deg, and altitude $h = 22,300$ ft. Only the static symmetric condition is studied, the modes used for this study are therefore the first bending and torsion mode only, and all asymmetric modes are disregarded. The high complexity of the aircraft model, together with the very nonlinear vortex flow being studied, requires very dense meshes for an accurate Navier–Stokes analysis of the *rigid* configuration. Then, adding to this, the complexity of a RANS aeroelastic analysis will present very severe challenges for the mesh deformation procedure for the fluid–structure interaction. This problem is relieved by running Edge in the inviscid mode for the aeroelastic solution. This inviscid aeroelastic solution determines the static deflection of the aircraft that can then be projected onto the Navier–Stokes mesh so that the RANS Edge analysis can be run in purely aerodynamic mode using the elastically deformed mesh. This is a reasonable approximation provided that the surface pressures computed in Euler and RANS modes are fairly similar (i.e., so that the deflections under these loads are similar).

A. CFD Code Edge

The aeroelastic CFD flow solver used in this study is Edge [16], a finite-volume Navier–Stokes solver for unstructured meshes. It employs local time stepping, local low-speed preconditioning, and multigrid and dual-time stepping for steady-state and time-dependent problems. The data structure of the code is edge-based so that the code is constructed as cell-vertex. It can be run in parallel on a number of processors to efficiently solve large flow cases. The Edge aeroelastic code provides functions for simulations with iterative coupling to an internal, modal, structural model. The movement of the CFD mesh is carried out in a procedure for quasi-elastic mesh deformation to enable mesh movement.

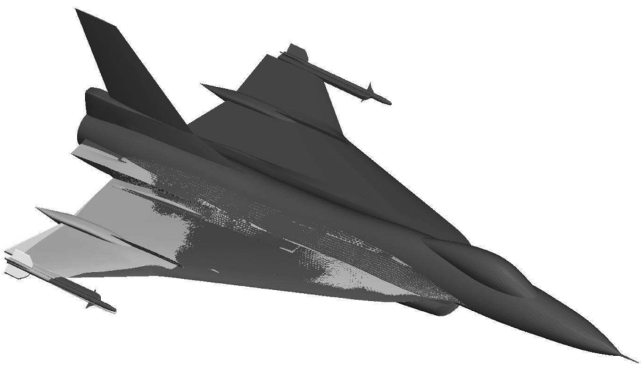

Fig. 6 Twist deformation on outboard wing due to aeroelasticity effects for FC70.

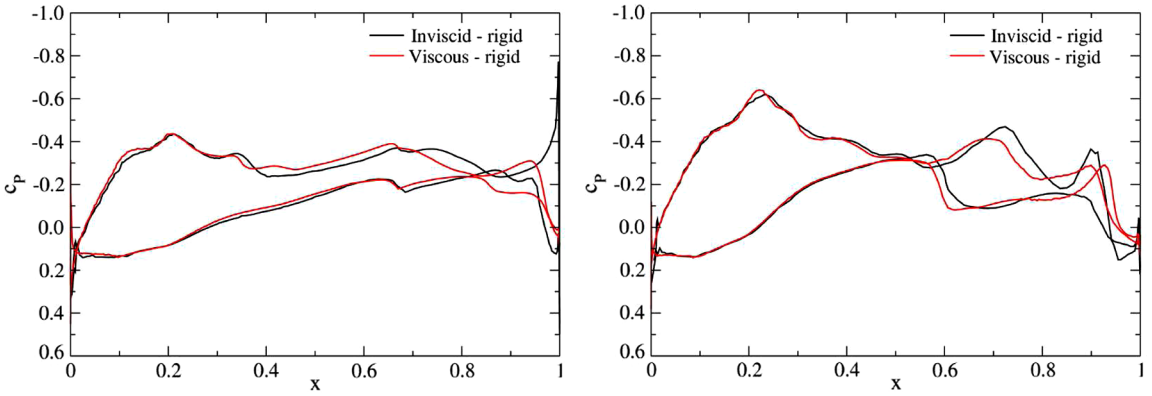

a) *BL*153 b) *BL*184

Fig. 7 Pressure distribution obtained by viscous and inviscid analysis of the rigid aircraft.

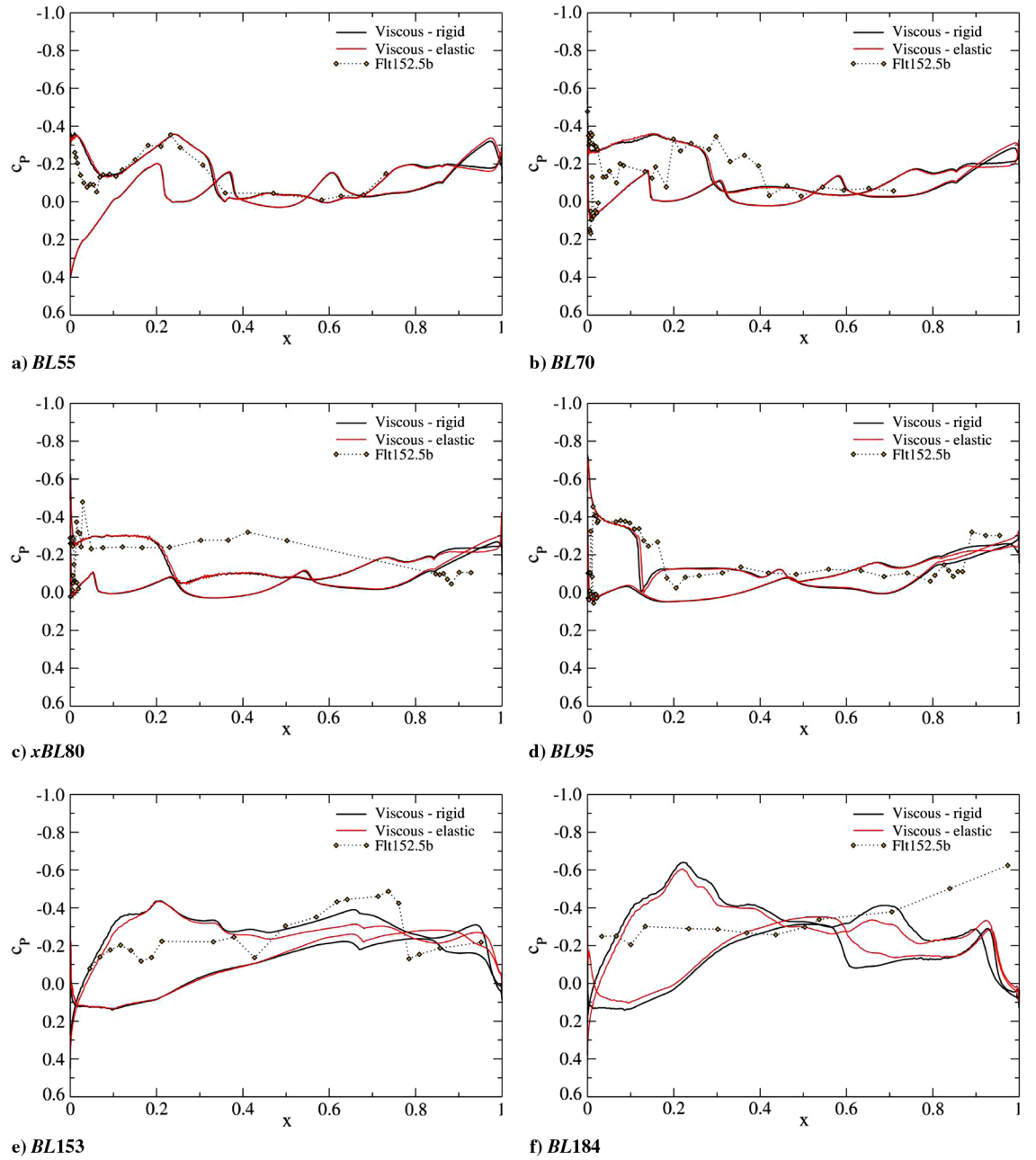

a) *BL*55 b) *BL*70

c) *xBL*80 d) *BL*95

e) *BL*153 f) *BL*184

Fig. 8 Rigid and elastic aircraft configuration, FC70.

The dynamics for small structural displacements can be accurately represented by a linear differential equation of the form

$$M\ddot{x} + C\dot{x} + Kx = f(t) \tag{1}$$

where $\boldsymbol{x}$ is the vector of structural coordinates, and $f(t)$ is the corresponding vector of forces. The M, C, and K are the mass, damping, and stiffness. The equation of motion can be reduced to the form

$$a_k\ddot{q}_k + 2\zeta_k a_k \omega_k \dot{q}_k = Q_k, \qquad k \in [1, N_m] \tag{2}$$

where ζ_k is the *damping ratio* for mode k and

$$Q_k = \phi_k^T f \tag{3}$$

is the corresponding generalized force. The structural damping matrix C is a linear combination of the mass and stiffness matrices M and K; that is, it is considered as a proportional or Rayleigh damping. The transformation of the load/displacements from CFD grid to FEM elements and vice versa is done using the radial basis functions interpolation, and the transformation matrix satisfies the energy conservation condition. The Edge aeroelastic solver was verified in code-to-code comparison using HIRENASD geometry [17].

The mesh used for the inviscid aeroelastic analysis had around 0.5 million surface triangles (around half the model) and contained 1,896,717 points, making 10.3 million tetra in the field.

The RANS mesh then that was deformed according to the computed static deflection contained 44 million points, making 68 million prism cells in 33 layers, 53 million tetra cells, and 0.6 million penta5 cells (cells connecting prisms and tetra cells) in the field. The final deformations were then used to deform the Navier–Stokes mesh around half model and calculate the pressure on elastic aircraft pressure RANS simulations. Figure 5 shows the surface mesh cells on the surface of the aircraft for viscous mesh.

These grids have come from a family of grids crafted and refined with much experience gained from past work on the F-16XL. See

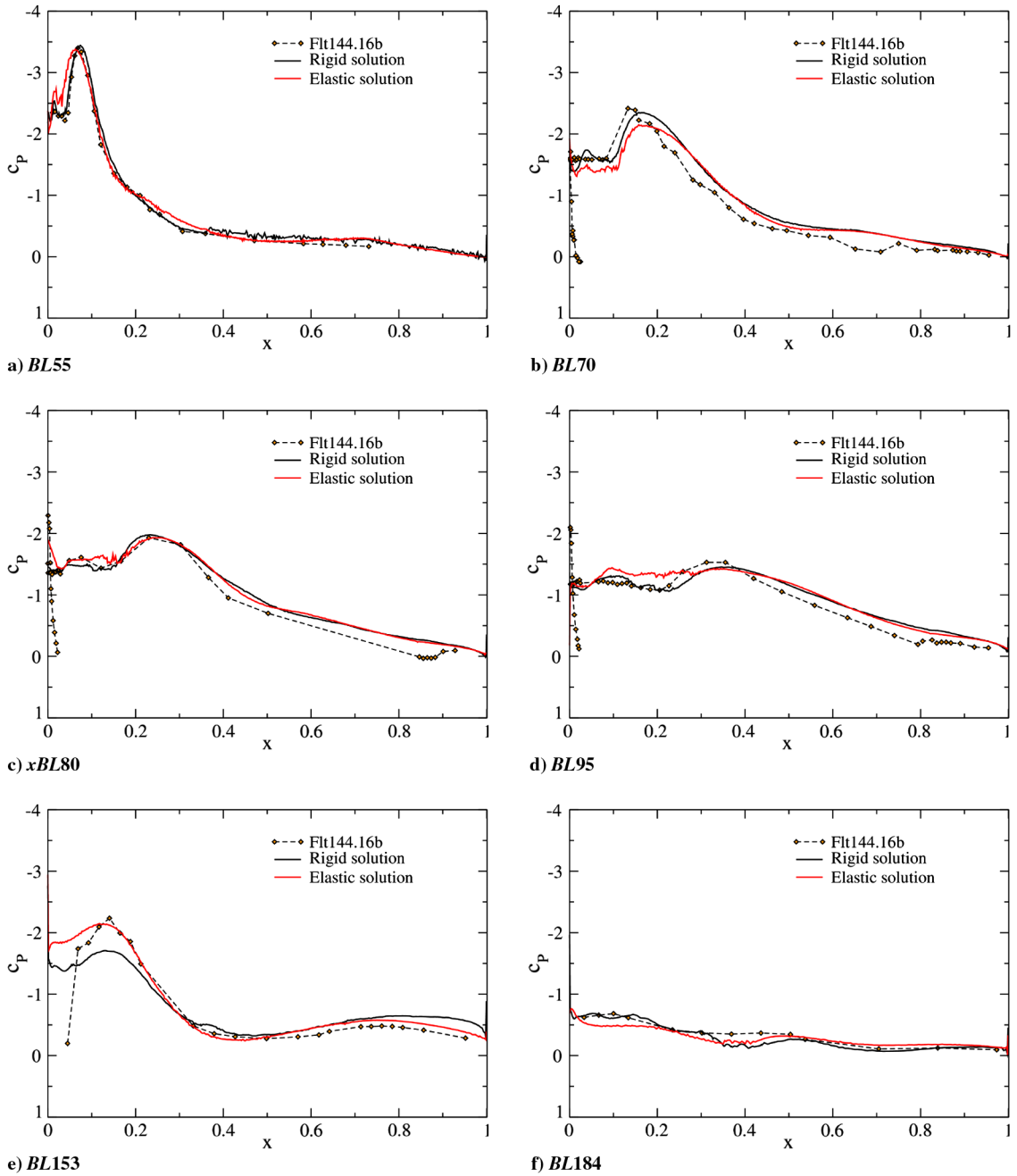

Fig. 9 Rigid and elastic aircraft configuration, FC25.

[18] for more information about this family of grids and how they have been used in CAWAPI-1 and CAWAPI-2.

B. FC70 Flight Condition

The flight condition FC70, which is a flight at Mach number $M = 0.97$, has long been investigated due to large discrepancies between the flight c_p and calculated c_p — see [3]. As shown in [3], the FC70 flight condition was the condition at which the variability between the different numerical solvers was the smallest one, yet the comparison to the flight data was the worst from all tested flight conditions.

The CAWAPI aircraft was calculated as a rigid and elastic aircraft using the inviscid analysis considering elastic effects in the Edge code, as explained above.

The approach of running aeroelastic analysis in inviscid mode and then using the predicted deformations to deform the Navier–Stokes mesh rather than running viscous aeroelastic analysis directly was chosen because of the excessive time that would be needed to run the URANS aeroelastic analysis, and the greater fragility of the mesh deformation procedure for such a dense URANS mesh. Figure 6 shows the static surface deformation due to aerodynamic loads on the wing. Notice the deformation of the advanced medium-range air-to-air missile (AMRAAM) missile around the nose. However, the influence of AMRAAM missile geometry on the aircraft aerodynamic is very limited.

The chosen methodology of running aeroelastic analysis in the inviscid mode and using the final deformations to make a new viscous mesh can be, however, used only if the pressure distribution and loads predicted by inviscid and viscous analysis are similar. To check this assumption, the pressure distributions were compared with each other. Figure 7 shows the pressure distribution on the outboard wing obtained by inviscid and viscous analysis on the rigid wing. The distributions are reasonably close to each other.

Figure 8 shows the pressure distribution on the rigid and elastic aircraft obtained by the RANS analysis.

Because of the stiffness of the inboard wing, the pressure distribution on the rigid and elastic aircraft is very similar to each other, and the outboard pressure distribution is affected primarily by the outboard wing twist. The difference between the rigid and elastic wing pressure distribution is largest at the *BL*184, which is the most outboard measured position.

Despite noticeable differences between the elastic and rigid wing pressure distributions, the final character of the pressure distribution in particular on the outboard wing panel suggests that the elasticity of the aircraft is *not* a source of the major discrepancy between the flight data and numerical simulations.

C. FC25 Flight Condition

Flight condition FC25 is a low-speed, high-angle-of-attack flight test case with conditions at Mach number $M_\infty = 0.242$, angle of attack $\alpha = 19.84$ deg, and altitude $h = 10,000$ ft. The dynamic loads on the aircraft are very similar to FC70 due to larger values of the lift and pitch moment coefficients and lower flight altitude, and thus the statically deformed RANS mesh for *FC70* was used for this case too. Figure 9 shows the pressure distribution on the rigid and elastic aircraft obtained by the RANS analysis. The results of aeroelastic analysis of this flight condition are similar to FC70 analysis; that is, the major effect of the elastic construction occurs on the outer wing panel, which is nicely visible particularly at position *BL*153, where the solution of elastic configuration matches flight data especially around the suction peak. The global character of the flow is though very similar to rigid aircraft.

V. Conclusions

This study aimed at assessing the effect of aeroelasticity on accuracy of the prediction of the flow around a military aircraft. The chosen geometry is the CAWAPI F-16XL delta wing aircraft previously studied in particular at higher angle of attacks and lower Mach numbers. Because the wings of fighter aircraft are usually stiff, the primary interests are cases with larger values of the dynamic pressure, FC70, and higher aerodynamic loads, FC25; however, each case is flight at $1g$.

The structural model used in this study is an approximation of likely structure of the real aircraft constructed using NeoCASS tool and based on publicly available information about the aircraft, such as the weight of the aircraft and ground vibration tests. The final structural model was provided with four modes, two symmetric and two asymmetric in bending and torsion. The two symmetric modes were used in the high-fidelity aeroelastic code Edge to assess the static aeroelastic deformation of the wing at the chosen fight conditions.

The high-fidelity CFD aeroelastic solver is Edge with a modal structural solver. The structural modes were projected on the surface using radial basis functions and the solver was run in the inviscid mode. The angle of attack was corrected so that the values of the lift correspond to the values of the lift predicted by the Navier–Stokes solution at given flight condition.

The aeroelastic approach was verified for the flight condition denoted FC70, which is a transonic flight condition at lower angle of attack, and for FC25, which is a low-speed, high-angle-of-attack flight condition. Both FC70 and FC25 have similar loads on the wing, meaning that the same elastic deformations can be used for both of them. The effects of the elastic structure of the aircraft on pressure distribution are moderate and occur mostly on the outboard wing panel. The results of aeroelastic simulations suggest that the character of the flow remains mostly similar to that of the rigid aircraft and that omission of the elastic construction during previous studies was *not* a source of discrepancies between CFD and flight data.

The result that the aeroelastic effects for the two flow conditions were found to be very small is not surprising because both cases are at $1g$. However, this validated the aeroelastic modeling for the $1g$ condition. A more interesting case would be a $3g$ transonic condition, for which the deflections would be much higher. Such a case is FC79 at $3.7g$, which was also investigated by Boelens and by Tomac et al. [5,18]. Their CFD results showed higher suction levels mainly on the outboard 50 deg swept panel as compared with flight data. Such differences are typical of an additional wing-tip panel nose-down twist. This is an expected result for the rigid panel because most of the aeroelastic effects for $3.7g$ would be concentrated on that structure in contrast to the much stiffer main inboard wing. Although this would be an interesting case to study aeroelastically, the inviscid-RANS procedure used here would probably breakdown for it because the FC79 case is high alpha and the difference in surface pressures between inviscid and RANS analysis could be large. Nonetheless, it is high g conditions where one must expect significant aeroelastic effects.

References

[1] Lamar, J. E., and Obara, J., "Review of Cranked-Arrow Wing Aerodynamics Project: Its International Aeronautical Community Role," *45th AIAA Aerospace Sciences Meeting and Exhibit*, AIAA Paper 2007-487, 2007.

[2] Obara, C. J., and Lamar, J. E., "Overview of the Cranked-Arrow Wing Aerodynamics Project International," *Journal of Aircraft*, Vol. 46, No. 2, March–Aug. 2011, pp. 355–368. doi:10.2514/1.34957

[3] Rizzi, A., Jirásek, A., Lamar, J. E., Crippa, S., Badcock, K. J., and Boelens, O. J., "Lessons Learned from Numerical Simulations of the F-16XL Aircraft at Flight Conditions," *Journal of Aircraft*, Vol. 46, No. 2, March–April 2009, pp. 423–441. doi:10.2514/1.35698

[4] Boelens, O. J., Badcock, K. J., Görtz, S., Morton, S., Fritz, W., Karman, S. L., Michal, T., and Lamar, J. E., "Description of the F-16XL Geometry and Computational Grids Used in CAWAP," *Journal of Aircraft*, Vol. 46, No. 2, March–April 2009, pp. 369–376. doi:10.2514/1.34852

[5] Boelens, O. J., Badcock, K. J., Elmilgui, A., Abdol-Hamid, K. S., and Massey, S. J., "Comparison of Measured and Block Structured Simulations for the F-16XL Aircraft," *Journal of Aircraft*, Vol. 46, No. 2, March–April 2009, pp. 377–384. doi:10.2514/1.35064

[6] Görtz, S., Jirásek, A., Morton, S. A., McDaniel, D. R., Cummings, R. M., Lamar, J. E., and Abdol-Hamid, K. S., "Standard Unstructured Grid Solutions for CAWAPI F-16XL," *Journal of Aircraft*, Vol. 46, No. 2, March–April 2009, pp. 385–408. doi:10.2514/1.35163

[7] Fritz, W., Davis, M. B., Karman, S. L., and Michal, T., "RANS Solutions for the CAWAPI F-16XL Using Different Hybrid Grids," *Journal of Aircraft*, Vol. 46, No. 2, March–April 2009, pp. 409–422. doi:10.2514/1.35106

[8] Luckring, J., Rizzi, A., and Smith, B., "Toward Improved CFD Predictions of Slender Airframe Aerodynamics Using the F-16XL Aircraft (CAWAPI-2)," *Journal of Aircraft* (to be published).

[9] Cavagna, L., Ricci, S., and Riccobene, L., "Structural Sizing, Aeroelastic Analysis, and Optimization in Aircraft Conceptual Design," *Journal of Aircraft*, Vol. 48, No. 6, Nov.–Dec. 2011, pp. 1840–1855. doi:10.2514/1.C031072

[10] Lamar, J. E., Obara, C. J., Fisher, B. D., and Fisher, D. F., "Flight, Wind-Tunnel, and Computational Fluid Dynamics Comparison for Cranked Arrow Wing (F-16XL-1) at Subsonic and Transonic Speeds," NASA TP-2001-210629, Feb. 2001.

[11] Lamar, J. E., "Cranked Arrow Wing (F-16XL-1) Flight Flow Physics with CFD Predictions at Subsonic and Transonic Speeds," RTO MP-069, 2001, p. 44.

[12] Riccobene, L., and Ricci, S., "Coupling Equivalent Plate and Beam Models at Conceptual Design Level," *Aircraft Engineering and Aerospace Technology*, Vol. 87, No. 1, 2015, pp. 2–10. doi:10.1108/AEAT-03-2013-0055

[13] Voracek, D. F., "Ground Vibrations and Flight Flutter Tests of the Single-Seat F16XL with a Modified Wing," NASA TM-104264, June 1993.

[14] Kim, T. S., and Kim, Y. Y., "Mac-Based Mode-Tracking in Structural Topology Optimization," *Computers and Structures*, Vol. 74, No. 3, Oct. 2000, pp. 375–383. doi:10.1016/S0045-7949(99)00056-5

[15] Eldred, M. S., Venkayya, V. B., and Anderson, W. J., "Mode Tracking Issues in Structural Optimization," *AIAA Journal*, Vol. 33, No. 10, Oct. 1995, pp. 1926–1933. doi:10.2514/3.12747

[16] Eliasson, P., "EDGE, a Navier–Stokes Solver for Unstructured Grids," *Proceedings of to Finite Volumes for Complex Applications III*, The Royal Aeronautical Soc., International Forum of Aeroelasticity and Structural Dynamics (IFASD) Paper 2013-004, 2002, pp. 527–534.

[17] Chwalowski, P., Heeg, J., Dalenbring, M., Jirasek, A., Ritter, M., and Hansen, T., "Collaborative HIRENASD Analysis to Eliminate Variations in Computational Results," International Forum of Aeroelasticity and Structural Dynamics (IFASD) Paper 2013-1D, Bristol, U.K., June 2013.

[18] Tomac, M., Jirasek, A., and Rizzi, A. W., "Factors Influencing Accurate Shock-Vortex Interaction Prediction on F-16XL Aircraft," AIAA Paper 2014-0420, 2014.